nature communications

Article

https://doi.org/10.1038/s41467-025-59772-5

Selective radical-type perfluoro-*tert*-butylation of unsaturated compounds with a stable and scalable reagent

Received: 13 February 2025

Accepted: 5 May 2025

Published online: 14 May 2025

Check for updates

Ruitong Zhang[1], Shengqi Zhou[2], Yijing Li[1], Yaxing Wu[1], Xiangyu Chen[1], Fei Wang[1], Yunchen Jiang[1], Xingwei Guo[2,3] ✉ & Chao Chen[1] ✉

Despite the promising potential of the perfluoro-*tert*-butyl group in diverse fields such as magnetic resonance imaging, material science and drug design, incorporating this group into organic molecules is still a formidable task, primarily due to its bulky structure and unique fluorine effect. Herein, we describe a stable and scalable reagent for radical-type perfluoro-*tert*-butylation, which is synthesized in large scale from commercial perfluoro-*tert*-butanol and a designed benzothiazole hypervalent iodonium salt. Highly *E*-selective photo-driven C(sp^2)–H functionalization of styrene derivatives is achieved in a triplet-triplet energy transfer halted manner, while thermally disfavored *Z*-products are also accessible by removing the energy antagonist. The application of this method is further demonstrated by late-stage functionalization and divergent synthesis of perfluoro-*tert*-butylated compounds.

Over the past two decades, fluoroalkylation reactions have garnered extensive research interest[1,2] owing to their promising applications in the fields of pharmaceuticals, agrochemicals, and functional materials[3–5]. Perfluoro-*tert*-butyl (PF*t*B) group, characterized by its exceptional structural bulkiness and robust electron-withdrawing capacity[6,7], stands out as an extreme example within the realm of fluoroalkyl groups. More importantly, PF*t*B-containing compounds exhibit considerable promise in magnetic resonance imaging (MRI)[8–10], material science[11] and drug design[12] (Fig. 1), which significantly amplifies their importance and potential applications. For example, PF*t*B labeling offers an efficient tool for monitoring RNA conformational behavior[9] (Fig. 1, left one) and PERFECTA[10] (Fig. 1, left two) is proven to possess excellent cellular compatibility, relaxation times and sensitivity for in vivo ^{19}F-MRI applications. As a result, the effect of introducing PF*t*B into molecules is much more than introducing a super CF_3 to simply alter the physical and biological properties.

Despite significant value demonstrated by PF*t*B-containing compounds has been shown across various fields, synthetic methodologies for incorporating PF*t*B into organic molecules remain limited and challenging. Traditionally, indirect ways are employed to synthesize PF*t*B-containing compounds, which demand limited commercial PF*t*B motifs[9,13–15], such as $(CF_3)_3COH$ and $(CF_3)_3CC\equiv CH$, or pre-functionalized substrates[16,17] (Fig. 2a). Though direct perfluoro-*tert*-butylation is highly appealing to chemists, it is still far from well-developed. In 1972, anion-type perfluoro-*tert*-butylation of organic compounds was firstly reported using highly toxic perfluoro-*iso*-butene[18]. Recently, Hu et al. modified this method to generate $(CF_3)_3C^-$ species elegantly[19,20] (Fig. 2b), while methods to introduce PF*t*B into universal substrates were still unreported. Given the intrinsic properties of $(CF_3)_3C^-$, namely its weak nucleophilicity, electron deficiency, substantial steric hindrance and instability, anion-type perfluoro-*tert*-butylation encounters significant constraints. These constraints manifest as incompatibility with transition metal catalysis and the necessity for highly reactive substrates, such as alkyl halides and arynes[19,20] (Fig. 2b), making perfluoro-*tert*-butylation different from well-established trifluoromethylation.

Correspondingly, radical-type perfluoro-*tert*-butylation has been much less studied, probably due to the scarcity of practical reagents to provide $(CF_3)_3C^{\cdot}$, a notable electrophilic carbon-centered radical[21,22].

[1]Key Laboratory of Bioorganic Phosphorus Chemistry & Chemical Biology (Ministry of Education), Department of Chemistry, Tsinghua University, Haidian, Beijing 100084, PR China. [2]Center of Basic Molecular Science (CBMS), Department of Chemistry, Tsinghua University, Haidian, Beijing 100084, PR China. [3]Present address: Department of Chemistry, and Center for Advanced Light Source, Southern University of Science and Technology, Shenzhen 518055, PR China. ✉e-mail: guoxw@sustech.edu.cn; chenchao01@mails.tsinghua.edu.cn

https://doi.org/10.1038/s41467-025-59772-5

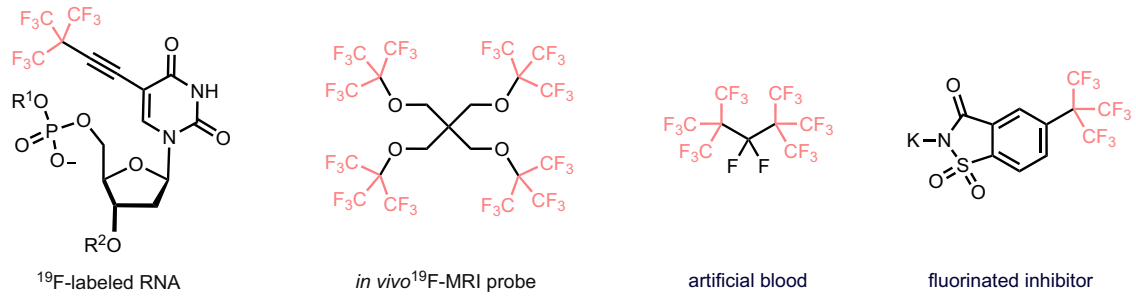

Fig. 1 | Selected examples of PF*t*B-containing compounds. PF*t*B-containing compounds show great potential in material science, drug discovery and magnetic resonance imaging.

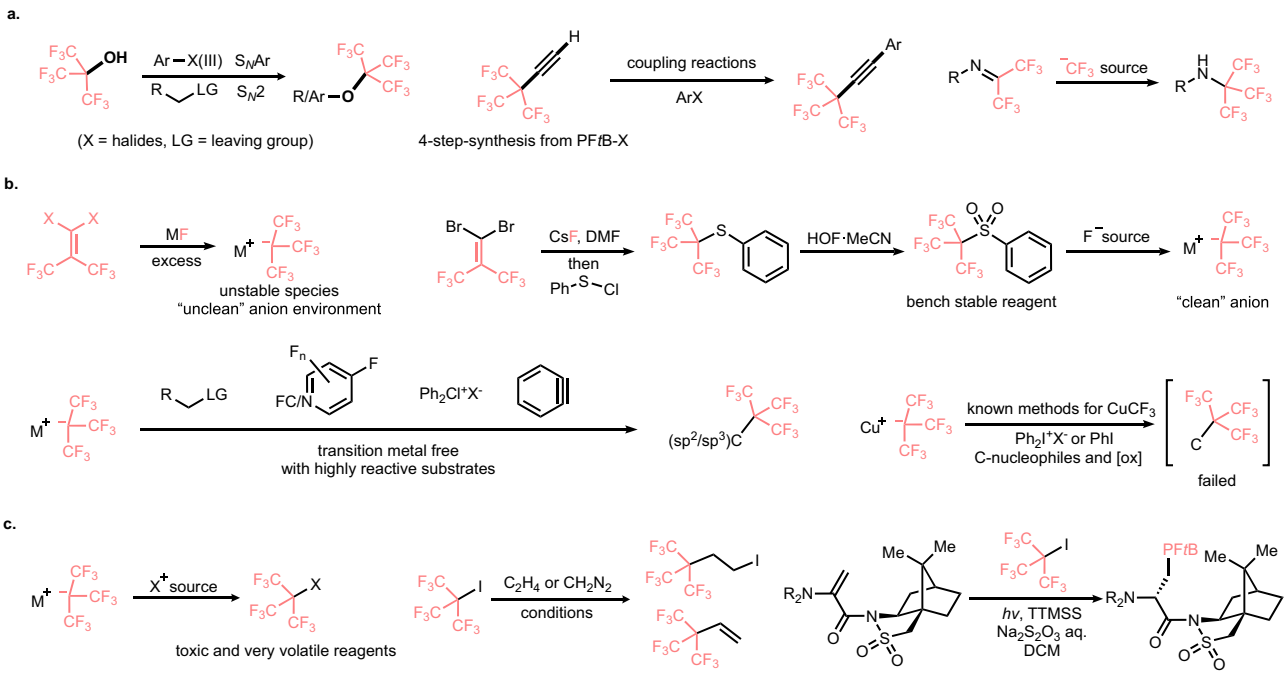

Fig. 2 | Synthetic methods for PF*t*B-containing compounds. a Indirect ways to introduce PF*t*B. **b** Reagents and reactions for anion-type perfluoro-*tert*-butylation. **c** Synthesis of PF*t*B-halides and their use in radical-type perfluoro-*tert*-butylation.

PF*t*B halides (Fig. 2c, left), sole known sources of $(CF_3)_3C^·$, were proven to generate $(CF_3)_3C^·$ under conditions like photolysis. However, these halides suffer from poor synthetic economy, inherent toxicity and instability, making radical-type perfluoro-*tert*-butylation still undeveloped (Fig. 2c, right, only two reported cases[23,24]). Consequently, there is a pressing need to develop novel reagents and reaction pathways for radical-type perfluoro-*tert*-butylation.

Deoxygenative coupling of alcohols has recently attracted considerable attention[25–28], primarily due to the broad accessibility of alcohols in comparison to other radical precursors. In this regard, developing reagents from $(CF_3)_3COH$, a bulk chemical renowned for its stability, cost-effectiveness and low toxicity, is highly desirable yet challenging because of the low reactivity[29]. For example, pK_a value for $(CF_3)_3CO–H$, $(CF_3)_2HCO–H$, $(CH_3)_3CO–H$ and $(CH_3)_2HCO–H$ were 5.4, 9.3, 17.1 and 15.3, respectively[30,31], indicating the weak nucleophilicity of $(CF_3)_3CO^-$. As a result, $(CF_3)_3COH$ is commonly used as non-nucleophilic protonic solvent and $(CF_3)_3CO^-$ is a widely used counter anion of ionic liquids.

Usually, strong electrophiles are employed to match the low reactivity of $(CF_3)_3COH$[13–15], however, corresponding products of established methods are unable to release $(CF_3)_3C^·$. In our proposal, an equivalent of aza-aryl cation could serve as a precursor to an aza-arene with a $(CF_3)_3CO–$ group, in which the covalent linkage of $(CF_3)_3CO–$ would further facilitate the production of $(CF_3)_3C^·$ (Fig. 3a).

Our attempt to synthesize the proposed reagent through typical approaches all failed (see Supplementary Information, SI, section 1), which promoted us to look for more suitable solution, which was, developing more reactive yet stable reagents to match the weak nucleophilicity of perfluoro-*tert*-butanol. Basing on Zhao's work[15] and our longstanding interest in hypervalent iodine chemistry[32–34], we designed a class of highly reactive diaryliodonium salts as equivalents of aza-aryl cations (Fig. 3b, up). Probably due to the lack of proper synthetic methods[35–38] and the highly reactive nature of these species, these aza-aryl cation equivalents were still unreported[39].

After lots of failed attempts, we were pleased to find compound **2** could be obtained *via* a mild σ metathesis from commercially available PIFA and corresponding ArTMS. After highly selective substitution with $(CF_3)_3CO^-$ to generate compound **3**, reagent **4** (RPF*t*B) could be synthesized in large scale (Fig. 3b, down). (The structures of **2a** and **4** were confirmed undoubtedly by X-Ray diffraction analysis.) We found that RPF*t*B showed an irreversible reduction potential of −0.05 V in MeCN, versus SCE, indicating its plausible reduction under various conditions (SI, section 8).

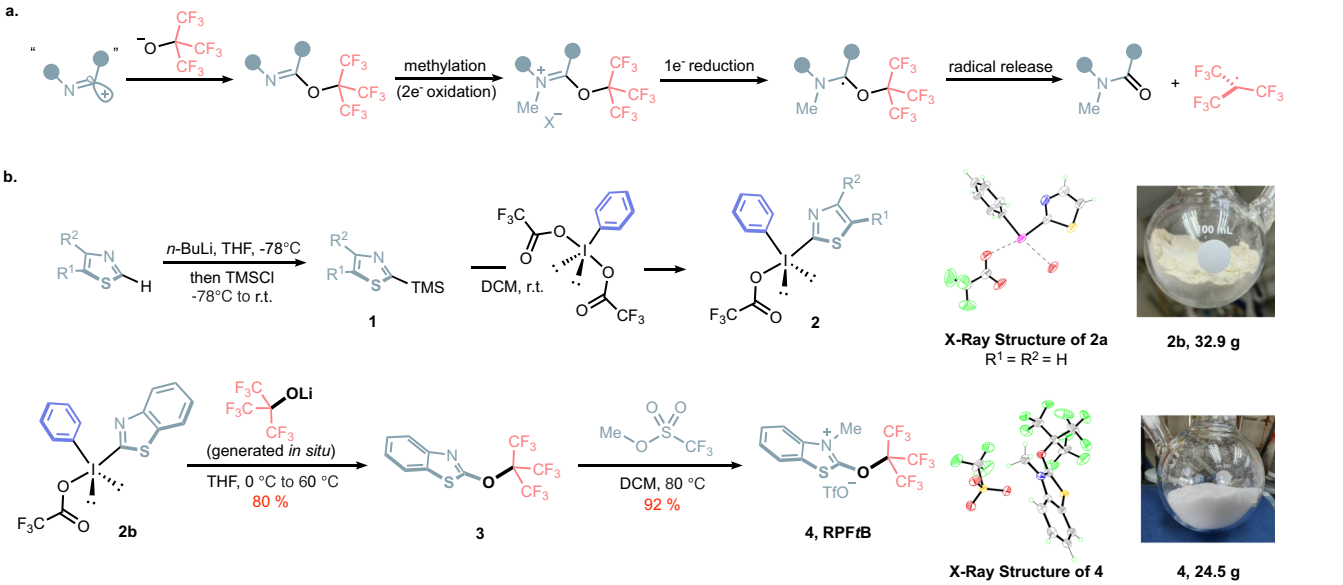

Fig. 3 | Design and synthesis of RPF*t*B. a Our proposal for developing reagents from perfluoro-*tert*-butanol. **b** Synthetic route for RPF*t*B.

In this article, we elucidate the utilization of RPF*t*B in the synthesis of PF*t*B-containing compounds via photocatalysis. Our findings reveal that single electron reduction of RPF*t*B efficiently releases $(CF_3)_3C^{\cdot}$, and this radical can be manipulated to participate in various catalytic cycles, leading to the production of diverse compounds. Concerning the difficulties illustrated by previous studies[19,20,23,24], radical perfluoro-*tert*-butylation basing on RPF*t*B provides an opportunity to access these valuable products in a practical way.

Results

Reaction development

Photocatalysis provides chemists opportunities to utilize transient species, especially radicals, into organic synthesis. Among numerous successes in this area, olefin chemistry stands as one of the most established fields through photo-driven radical pathways, leading to products with great diversity. As one of the most basic and important cases, photo-driven Heck-type reaction (vinyl C(sp^2)–H functionalization) has largely broadened the edge of the classical textbook reaction in both substrate capability and selectivity[40]. However, despite lots of successes have been made, developing photocatalytic methods for C(sp^2)–H functionalization of electron-deficient radicals is still challenging due to the lack of mild way to generate these radicals and re-establishment of unsaturation ensuing radical addition[41].

Considering PF*t*B substituted olefins' value in further transformation and the lack of synthetic methods, we were motivated to develop a general strategy for selective radical C(sp^2)–H perfluoro-*tert*-butylation. Styrene derivatives, which were challenging substrates for this photocatalytic reaction[42–44] with regard to plausible polymerization, isomerization through triplet-triplet energy transfer (TTET)[45,46] and dimerization[47], were chosen as our prototypical substrates. Investigation of the reaction conditions (see SI section 6 for detailed optimizations) suggested the best conditions listed in Fig. 4. We identified *fac*-Irppy$_3$ ($E_{1/2}$ (M^+/M*) = −1.73 V, versus SCE[48]) as an effective photocatalyst, together with CuTC as transition metal catalyst. For electron-deficient or electron neutral styrene derivatives, when the reaction was carried out in DCM under irradiation of blue LEDs (10 W and 425 nm), no additional base was needed to deliver corresponding *E*-alkene product in satisfying yield and selectivity (entry 1, 78%, *E*:*Z* > 20:1). In this case, the choice of base and solvent played a crucial role in determining *E*/*Z*-selectivity. The addition of several kinds of base would lead to a higher ratio of *Z*-isomer (entries 2 and 3) and similar phenomena was also found when using different solvents (entries 4 and 5). The initial valence and source of the copper catalyst would not influence the result, indicating both Cu(I) and Cu(II) catalyst were able to involve the catalytic cycle (entry 6). Conditions for electron-enriched styrene derivatives, which were easy to undergo acid-catalyzed polymerization, were studied by using *p*-Me substituted substrate. To our delight, when organic base D*t*BP (2,6-di-*tert*-butylpyridine) was added to adjusting the acidity, the yield significantly increased from 44% to 88% (entries 7 and 8). It was also surprising that, in comparison with entry 3, *p*-Me substituted product showed a lower tendency for photo-induced isomerization in the presence of base even in a longer time scale (entry 9), indicating that substitution effect played a crucial role in this isomerization. Change of photocatalyst would influence the yield and reaction would not take place under photocatalyst-free condition (entries 10 and 11). An obvious drop of yield was observed without copper catalyst (entry 12), indicating the importance of rate-matching in radical-polar crossover to compete with unproductive pathways.

With the optical conditions in hand, we next explored the scope and limitation of this radical perfluoro-*tert*-butylation (Fig. 5 and SI section 7). Previous studies on Ir-based photocatalyzed C(sp^2)–H functionalization showed that *E*/*Z*-selectivity suffered from position effect and electron effect of the substitutions due to the incontrollable TTET process, and method like flow chemistry was utilized to obtain better selectivity[42,44]. Thus, we were motivated to search for a general solution to gain good yield and selectivity for substrates with broad structural diversity.

Position effect was investigated by testing various halogen substitutions (**6b**-**6f**), which all gave excellent yields from 80% to 95% and high selectivities (*E*:*Z* > 20:1). Several electron-withdrawing substitutions, including halogens (**6g**-**6j**), an ester group (**6k**), a sulfone group (**6l**, CCDC2405100), an aldehyde group (**6m**), a cyano group (**6n**), perfluoroalkoxy groups (**6o** and **6p**) and a BPin group (**6q**) could be accommodated, furnishing products with satisfying results. Simple styrene (**6r**) and 1-/2-naphthylethylene (**6s** and **6t**) could also gave corresponding products, however, an obvious drop of selectivity occurred in the case of 1-/2-naphthylethylene. Substrates with a *tert*-butyl group (**6u**), methyl groups (**6v, 6w** and **6x**), a phenoxy group (**6y**), a methoxy group (**6z**) and an acetoxy group (**6aa**) could be transformed with reasonable results in the presence of D*t*BP to prevent

https://doi.org/10.1038/s41467-025-59772-5

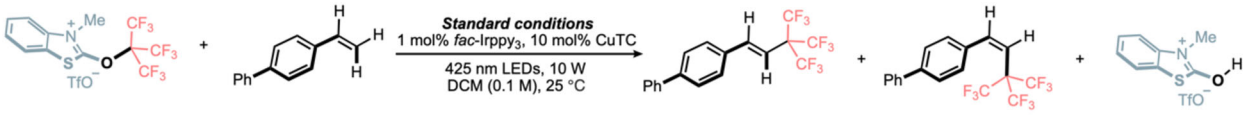

4, 1.2 equiv. **S.M. 5a**, 1.0 equiv. **6a** **7a** **8**, MBTO-HOTf

Entry	Variations from the standard conditions	Yield of *E*-product (%)	Yield of *Z*-product (%)	*E*:*Z* ratio
1	No	72	2	> 20:1
2	2 equiv. Cs_2CO_3 as base	1	78	< 1:20
3	2 equiv. D*t*BP as base	6	50	1:8.3
4	EtOAc instead of DCM	51	44	1.2:1
5	DMF instead of DCM	2	86	< 1:20
6	$Cu(OTf)_2$ instead of CuTC	68	3	> 20:1
7	S.M.: *p*-Me instead of *p*-Ph	44	1	> 20:1
8	S.M.: *p*-Me instead of *p*-Ph and 2 equiv. D*t*BP as base	88	3	> 20:1
9	S.M.: *p*-Me instead of *p*-Ph and 2 equiv. D*t*BP as base, 8 h	86	2	> 20:1
10	$Ru(bpy)_3(PF_6)_2$ instead of *fac*-Irppy$_3$	5	-	-
11	No *fac*-Irppy$_3$	-	-	-
12	No CuTC and 2 equiv. Cs_2CO_3	5	10	1:2.0

Fig. 4 | Optimization of reaction conditions. Selected entries for reaction optimization are listed. Reactions were done in 0.1 mmol scale. All the yields were determined by GC-MS analysis using *n*-dodecane as internal standard. Irradiation time was 4 h for reaction optimization unless otherwise noted.

polymerization. Internal alkynyl group (**6ab**) and chloromethyl group (**6ac**) were compatible in the system to show that the mild condition might be used in sensitive molecules.

1,2-diazole (**6ad**), thiazole (**6ae**) and pyridine (**6af**) were also tolerated to give yields from 38% to 70% and *E*:*Z* > 20:1. Late-stage functionalization of natural products and drug molecules modified with a styrene handle, such as febuxostat intermediate (**6ag**), naproxen (**6ah**), estrone (**6ai**), oxaprozin (**6aj**), sulbactam (**6ak**) and indomethacin (**6al**), could be transformed efficiently, thus conforming the generality of our conditions.

To further test the ability of our photochemical synthetic platform, different kinds of substrates were examined under slightly modified conditions (Fig. 6 and SI section 7). Following extensive screening of various radical reaction partners, we were pleased to find that phenylacetylene derivatives could be transformed to deliver PF*t*B substituted alkynes in moderate to good yields (**9a**–**g**)[49], which represented a rare example for C(sp)–H fluoroalkylation via radical mechanism[50]. Electron enriched aromatic compounds like acetanilide, benzothiophene, benzofuran and indole derivatives were also suitable partner in the catalytic cycle (**10a**–**f**). It was also notable that these perfluoro-*tert*-butylation reactions were highly regioselective (e.g., **10e**), indicating that both electronic and steric effect played an important role. Other common motifs, like 1,1-disubstituted alkene (with aryl substitutions, **11a**, with alkyl substitutions, **11b**), pyridine-derived 1,3-diene (**12**)[51,52] and silyl enol ether (**13**), were also reactive substrates under our conditions. However, unactivated arenes showed low conversions under our conditions and only strong electron-donating group could slightly promote the transformation to compete with unproductive pathways of PF*t*B radical. (SI, section 7)

The usefulness of RPF*t*B in organic synthesis was also demonstrated in other radical reactions. As shown in Fig. 7, under simply modified conditions, diverse compounds could be synthesized using RPF*t*B. By removing the copper catalyst, the alkyl radical intermediates could react with simple hydrogen donor (**14**)[42] or undergo intramolecular cyclization (**15a, 15b**)[53] to obtain difunctionalized products. Also, the hypervalent organo-copper species could undergo C–N (**16**) or C–O (**17**) reductive elimination to form cyclic products[54]. These findings largely extended the applicability of our platform.

Mechanism study

To gain a deeper understanding of the reaction mechanism, TREPR experiments were conducted, and the key intermediate was directly characterized using our recently developed ultrawide single sideband phase-sensitive detection (U-PSD) time-resolved electron paramagnetic resonance (TREPR) technique[55]. The measurements were performed with a simplified reaction system consisting of RPF*t*B (10 mM) and Ir[dF(CF_3)ppy]$_2$(dtbbpy)PF_6 (1 mM).

The reaction was triggered *via* photoinduced electron transfer between Ir(III)* and RPF*t*B with an excitation wavelength of 450 nm. To our delight, a radical intermediate with a lifespan of 400 μs was observed (see SI, Fig. S21). A transient EPR spectrum centered at g = 2.0028 was successfully acquired by integrating the signals between 1–10 μs after the laser pulse, showing a well-resolved splitting pattern (9 a_F = 1.84 mT) (Fig. 8a), which aligned well with $(CF_3)_3C^{\cdot}$ of literature reports[22]. Under reaction condition with a higher concentration (50 mM) of RPF*t*B, the expected carbon-centered radical generated via single-electron transfer from the Ir(III)* catalyst to RPF*t*B, was not directly observed. This suggested that the β-scission rate was extremely fast, which nearly occurred within a time window close to the instrumental resolution limit (40 ns), indicating that the rate constant must exceed 10^7 s^{-1} (see SI in detail, Fig. S22).

After proving RPF*t*B's ability to deliver $(CF_3)_3C^{\cdot}$ under our photocatalytic condition, radical clock experiment was carried out to investigate the behavior of this electrophilic and sterically hindered radical. **18** was treated under our standard conditions (Fig. 8b) to afford cyclopropyl ring opened products **19** and **20**, which indicated a free radical addition process[21] without the formation of CuR_f. Our initial optimization showed an obvious drop of yield under copper-free condition, which might be attributed to the incompatible rate of benzyl radical oxidation (by Ir(IV), $E_{1/2}$ (M^+/M) = +0.77 V)[48], and

https://doi.org/10.1038/s41467-025-59772-5

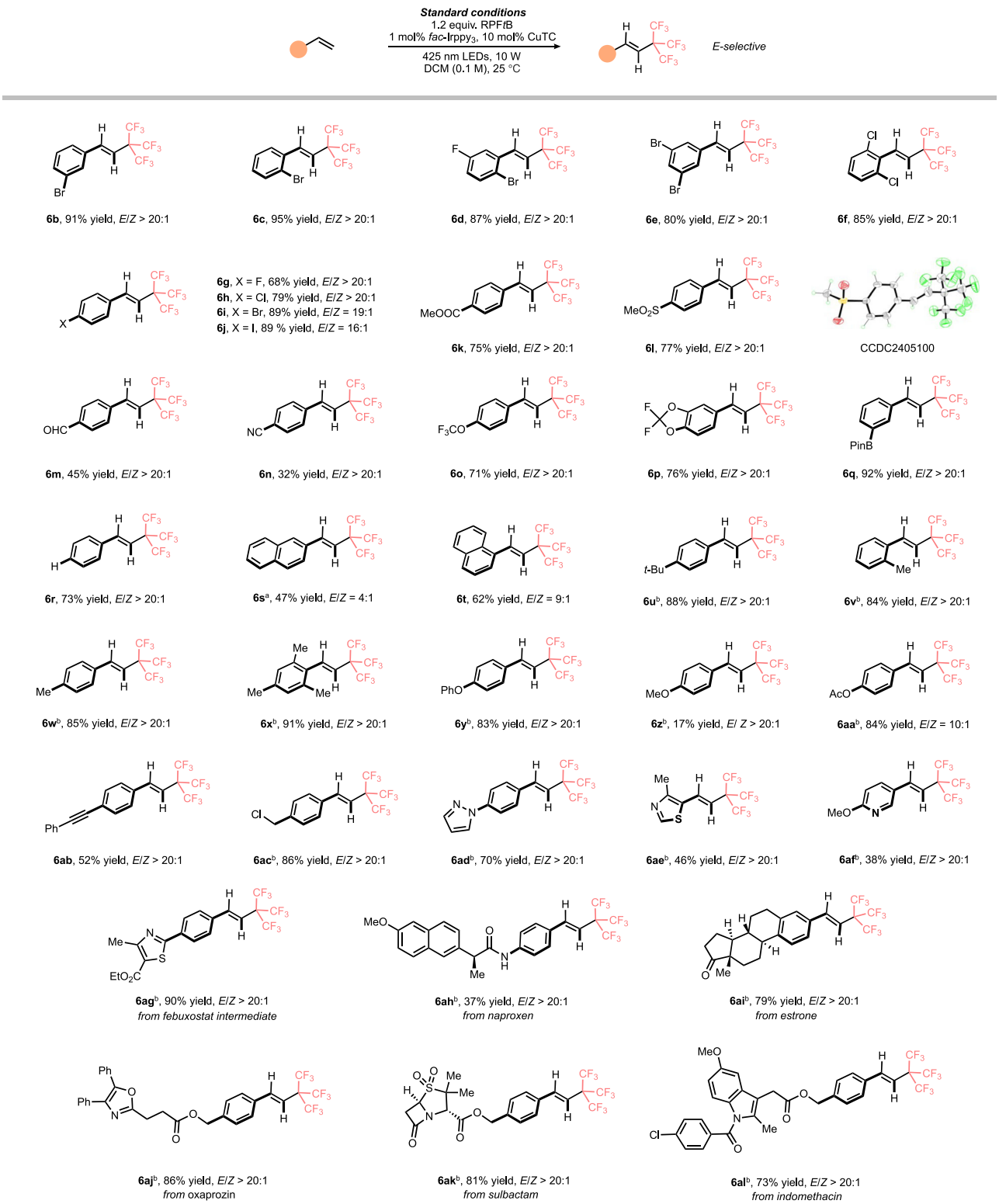

Fig. 5 | Scope for *E*-selective C(sp^2)–H perfluoro-*tert*-butylation of styrene derivatives. The reaction shows excellent functional group tolerance and is compatible in late-stage functionalization. Reactions were done in 0.2 mmol scale using standard conditions unless otherwise noted. All the yields above were isolated yields for *E*-isomer. **a** 2 equiv. $CaCO_3$ was added as base. **b** 2 equiv. D*t*BP was added as base.

unproductive pathways like radical polymerization or HAT (from the solvent) would be favored. When the benzyl radical was trapped by Cu(II) catalyst to form organocopper(III) intermediate[56], β-H elimination would occur to deliver PF*t*B substituted olefins.

DFT calculations were done at the TPSS-D3/def2-TZVP//TPSS-D3/def2-SVP level to give insights into the selectivity of β-H elimination[57]. As shown in Fig. 8c, there was a 13.4 kcal/mol energy gap between two configurations of PF*t*B substituted organocopper species (blue lines) **int 1** and **int 2**, which was caused by the steric repulsion. Similar energy gap for CF_3 substitution was 5.6 kcal/mol, a much lower barrier for σ rotation process. The energy difference for concerted *Z*- and *E*-selective elimination was −3.3 kcal/mol (G_{ts2}–G_{int2}–G_{ts1}+G_{int1}) in the

https://doi.org/10.1038/s41467-025-59772-5

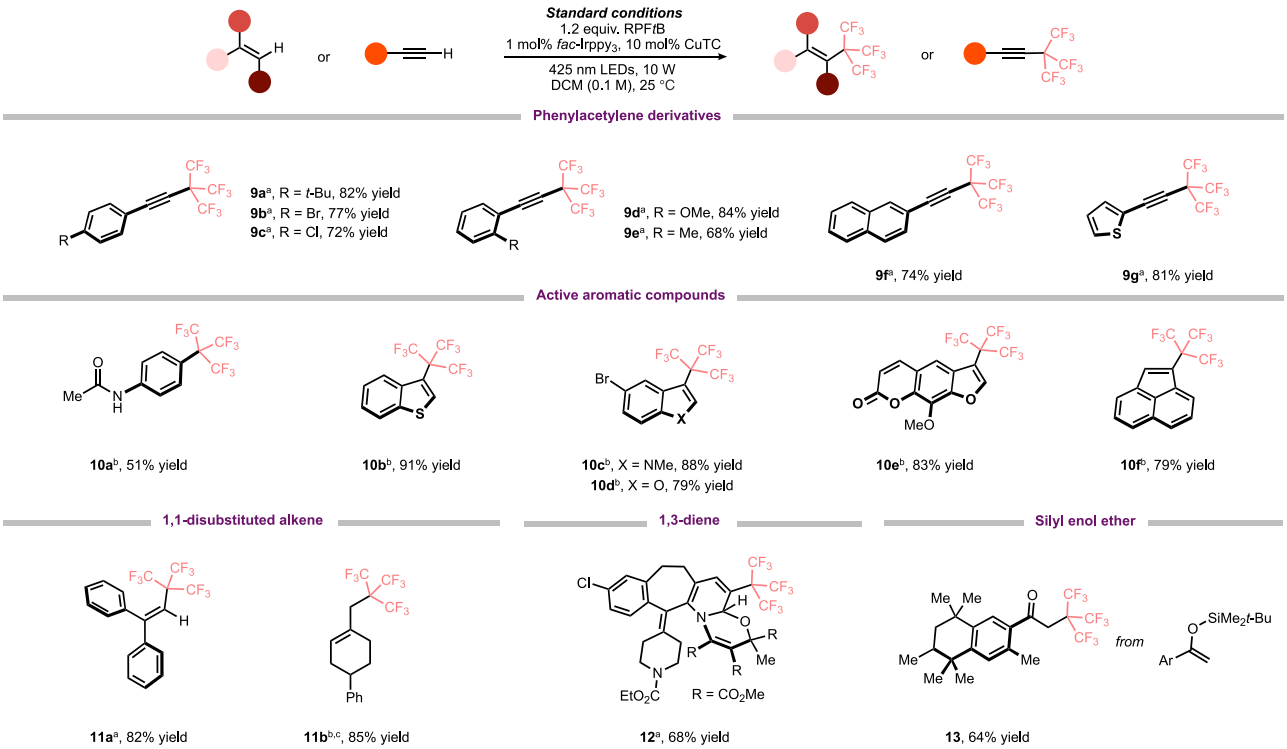

Fig. 6 | Broader scope for C–H perfluoro-*tert*-butylation of unsaturated compounds. Unsaturated compounds including alkynes and electron-enriched aromatic compounds are also good reaction partners under slightly modified conditions. Reactions were done in 0.2 mmol scale using standard conditions unless otherwise noted. All the yields above were isolated yields. **a** 2 equiv. Na_2CO_3 was added as base. **b** 2 equiv. D*t*BP was added as base. **c** DMF as solvent.

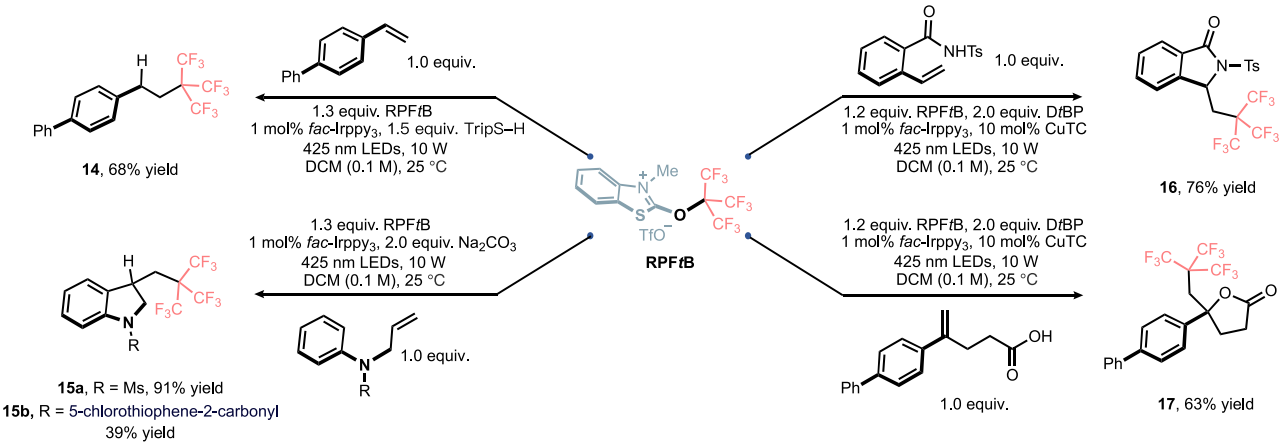

Fig. 7 | Extension of the platform for diverse synthesis of olefin substrates. RPF*t*B's application in difunctionalization and tandem cyclization of unsaturated compounds. For reaction details, see SI section 7.

case of PF*t*B, however, −1.1 kcal/mol for CF_3, indicating the higher steric repulsion in both **int 2** and **int 2'** would slightly enhance the *Z*-selective elimination. The energy provided by DFT suggested *E*-selective elimination was much favored due to the decisive σ rotation process and the *Z*-selectivity observed in our condition (Fig. 1, entry 2) was not caused by weak intramolecular interaction such as C–H···F hydrogen bond.

In order to show the details of *E*/*Z* isomerization, a mixture of **6a** and **7a** was treated with different conditions listed in Fig. 8d. When the olefin together with the photocatalyst was exposed to blue LEDs for 5 min, a fully conversion from **6a** to **7a** was detected and no loss of the olefin was observed. To prove the *E*-selectivity under no base additive conditions was not the result of acid-catalyzed thermo-isomerization *via* carbonium cation[58], the mixture was treated with excess amount of HOTf (SI, Table S7). It was found that, the strong acid led to a pot of messy crude probably because of the cationic polymerization, which promoted us to find a more suitable explanation for the selectivity. We were pleased to find that, the side product MBTO played a crucial role in the isomerization. Serving as an internal base in the system, MBTO would quench the HOTf to form MBTO-HOTf, which efficiently suppressed the isomerization in a competitive SET process[59]. In the presence of 1.0 equiv. MBTO-HOTf and ca. 3 mol% photocatalyst, the *E*:*Z* ratio could be remained even in longer time scale (4 h, from 35:65 to 30:70) without the loss of yield. Similar effect could also be found in the presence of D*t*BP-HOTf, however, with much lower efficiency (5 min, from 35:65 to 18:82).

https://doi.org/10.1038/s41467-025-59772-5

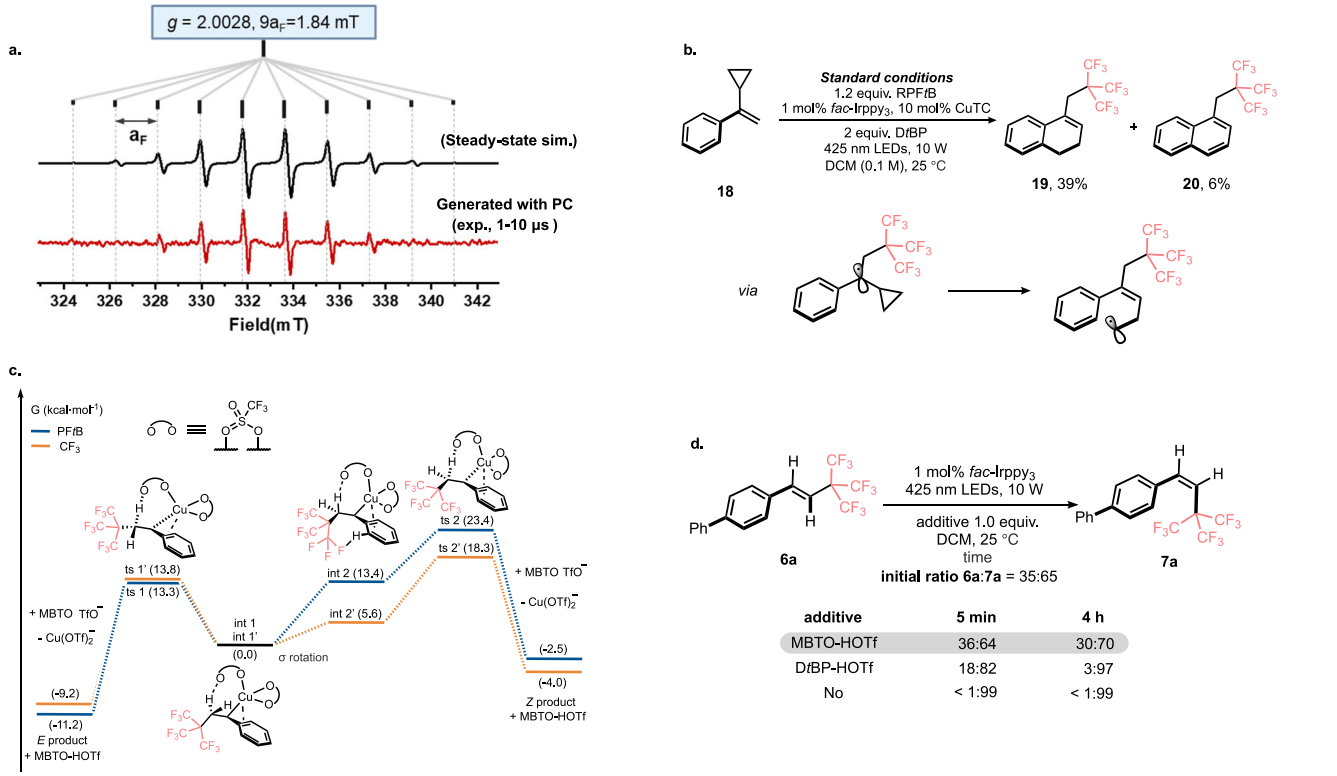

Fig. 8 | Mechanism studies. a U-PSD TREPR detection. **b** Radical clock experiment. **c** DFT calculation. **d** *E*/*Z* isomerization. See SI section 8 for details.

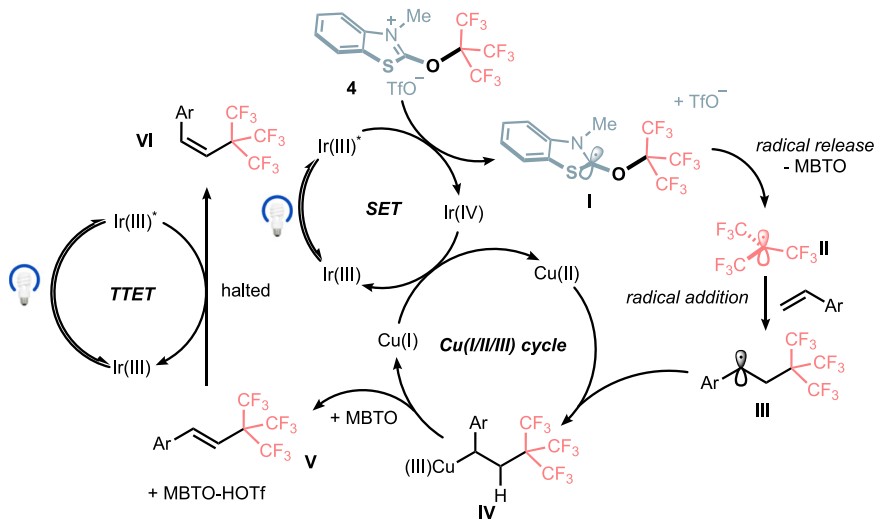

Fig. 9 | Proposed mechanism. An energy antagonist generated in situ is proposed to be the key for the *E*-selectivity.

Basing on the mechanism studies, the selective radical C(sp^2)–H perfluoro-*tert*-butylation of styrene derivatives is proposed to undergo the process described in Fig. 9. First, single electron transfer from the Ir(III)* catalyst to RPF*t*B can generate carbon radical intermediate **I**, which then undergoes fast C–O bond cleavage to release $(CF_3)_3C^{\cdot}$ **II**. Radical addition of **II** to an unsaturated bond affords intermediate **III**, which can be quenched by a H-donor or an intramolecular aromatic ring. When intermediate **III** is trapped by Cu(II) to form organo-copper(III) intermediate **IV**, *E*-selective β-H elimination occurs to generate product **V** and Cu(I). Efficient triplet-triplet energy transfer of **V** with Ir(III)* will produce *Z*-product **VI** following an irreversible manner. However, one equivalent of MBTO-HOTf (or base-HOTf) is generated along the elimination, which efficiently suppresses the TTET process and leads to the observed *E*-selectivity.

Z-Selective C(sp^2)–H perfluoro-*tert*-butylation of styrene derivatives

After fully studying the reaction mechanism, we were pleased to further test the efficiency of TTET-allowed selectivity-reversed reaction by removing the energy antagonist **8** (Fig. 10 and SI, section 8). Corresponding products, with a highly strained double bond caused by PF*t*B substitution, were not available by traditional methods.

We were glad to find that PF*t*B substituted styrene showed a complete conversion in 4 h, delivering corresponding thermally disfavored *Z*-isomer **7b** in 70% yield. Substrates with electron-withdrawing groups were less likely to isomerize regarding the trend shown in **7b** to **7e** (slower rate and lower conversion). *p*-*t*-Bu and *o*-Me substitutions would not influence the conversion (**7f** and **7 g**), while 2,4,6-trimethyl substrate showed much lower yield even in longer time

https://doi.org/10.1038/s41467-025-59772-5

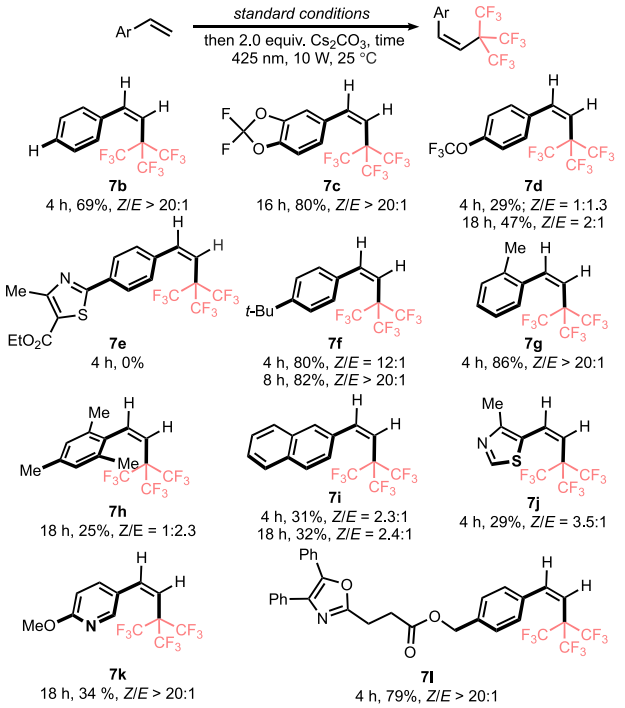

Fig. 10 | Scope for *Z*-selective C(sp^2)–H perfluoro-*tert*-butylation of styrene derivatives. *Z*-Selective perfluoro-*tert*-butylations of styrene derivatives are performed under modified conditions. Yields for *Z*-isomers were given. For details, see SI, section 8.

scale (**7h**), probably owing to triplet energy difference caused by the weaker conjugation and the unignorable steric effect. 1-Naphthyl substrate, with expanded π system, was less effective in this transformation (**7i**). Substrates basing on thiazole and pyridine cores were also examined (**7j** and **7k**), showing good to excellent conversion. Finally, oxaprozin derived substrate was tested (**7l**) to show orthogonality of isolated π system (an ester group and a diphenyloxazole) to this photoinduced isomerization.

Above results indicated that the Ir-catalyzed TTET process was widely feasible in our system and further highlighted the importance of our energy antagonist strategy in selectivity control, so that we could achieve this unusual tunable C(sp^2)–H perfluoro-*tert*-butylation.

Discussion

In summary, we have developed a stable and scalable reagent for radical-type perfluoro-*tert*-butylation. The precursors of the reagent (hypervalent iodine(III) reagent and perfluoro-*tert*-butanol) are either commercially available or easy handling, making the synthesis of the reagent highly applicable. The reagent is proven to release $(CF_3)_3C^{\cdot}$ under single electron reduction condition, and a diverse synthetic platform for perfluoro-*tert*-butylation of unsaturated compounds, such as alkenes, alkynes and electron enriched aromatic compounds, are built by photocatalysis. Notably, both *E*- and *Z*-selective C(sp^2)–H perfluoro-*tert*-butylation of styrene derivatives could be achieved through a controllable TTET process, owing to the unique property of our reagent. Our work largely extends the diversity and applicability of PF*t*B-containing compounds and will gain broad interest in related research fields, such as hypervalent iodine chemistry, fluorine chemistry, photocatalysis and magnetic resonance imaging.

Methods

General procedure for the synthesis of 2b

To a 250 mL oven-dried flask with a magnetic stirring bar, PIFA (43.0 g, 100 mmol, 1.0 equiv.), anhydrous DCM (100 mL) were added. Then compound **1b** (22.5 g, purity = 92%, ca. 100 mmol, 1.0 equiv.) was added dropwise to the mixture at room temperature. The mixture was allowed to stir at room temperature for another 2 h after the solid (PIFA) completely disappeared and the solution turned brown. 100 mL pre-cooled (−20 °C) pentane was added to the solution and the flask was cooled to −20 °C. The cooled mixture was then filtered and the white cake was quickly washed with pre-cooled pentane (3×30 mL). The cake was dried in vacuo providing compound **2b** as an off-white solid (32.9 g, 73% isolated yield).

Note: ***The cake should be washed quickly because the brown impurity would lead to the decomposition to form black oil.***

General procedure for the synthesis of 3

To a 250 mL oven-dried flask with a magnetic stirring bar, perfluoro-*tert*-butanol (19.6 g, 83 mmol, 1.14 equiv.), anhydrous THF (100 mL) were added under nitrogen atmosphere. Then the solution was cooled to 0 °C. Then *n*-BuLi (2.5 M in hexane, 31.2 mL, 78 mmol, 1.07 equiv.) was dropped into the mixture. The mixture was stirred at 0 °C for 10 min. Then compound **2b** (32.9 g, 73 mmol, 1.0 equiv.) was added and the mixture was allowed to heat to 60 °C and stirred for 24 h. The solvent was removed under reduced pressure and the crude was purified by flash chromatography (petroleum ether to petroleum ether/ethyl acetate = 200/1) to provide compound **3** as a white solid (21.6 g, 80% isolated yield).

General procedure for the synthesis of 4 (RPF*t*B)

To a 250 mL oven-dried sealed tube with a magnetic stirring bar, compound **3** (18.5 g, 50 mmol, 1.0 equiv.), anhydrous DCM (50 mL), MeOTf (10.7 g, 65 mmol, 1.3 equiv.) were added under nitrogen atmosphere. Then the solution was heated to 80 °C and stirred for 18 h. The tube was cooled to room temperature and 30 mL pre-cooled Et_2O (−20 °C) was added. The cooled mixture was then filtered and the white cake was washed with pre-cooled Et_2O (3×30 mL). The cake was dried in vacuo providing compound **4** as a white solid (24.5 g, 92% isolated yield).

General procedure for the perfluoro-*tert*-butylation

Under an ambient atmosphere, in a 25 mL Schlenk tube equipped with a magnetic stirring bar, S.M. (starting material, 1.0 equiv.), **4** (1.2 equiv.), *fac*-Irppy$_3$ (1 mol%) and CuTC (10 mol%) (and 2.0 equiv. of base if needed) were dissolved in degassed DCM (0.1 M). The tube was irradiated at blue LEDs (425 nm, 10 W), 25 °C for different time depending on the substrate. The solvent was removed under reduced pressure (15 °C to 35 °C) and the crude was purified by flash chromatography. No special work-up procedure was needed unless otherwise noted.

Data availability

Crystallographic data for compound **2a**, **4** and **6l** have been deposited at the Cambridge Crystallographic Data Centre under deposition number no. CCDC2405101 (compound **2a**), CCDC2405099 (compound **4**) and CCDC2405100 (compound **6l**). Copies of the crystal data can be obtained free of charge *via* www.ccdc.cam.ac.uk/data_request/cif. All these data are available in the main text and supplementary files, or from the corresponding author upon request. Source data are provided with this paper.

References

1. Ni, C. & Hu, J. The unique fluorine effects in organic reactions: recent facts and insights into fluoroalkylations. *Chem. Soc. Rev.* **45**, 5441–5454 (2016).
2. Qing, F.-L., Liu, X.-Y., Ma, J.-A., Shen, Q., Song, Q. & Tang, P. A fruitful decade of organofluorine chemistry: new reagents and reactions. *CCS Chem* **4**, 2518–2549 (2022).
3. Purser, S., Moore, P. R., Swallow, S. & Gouverneur, V. Fluorine in medicinal chemistry. *Chem. Soc. Rev.* **37**, 320–330 (2008).

4. Muller, K., Faeh, C. & Diederich, F. Fluorine in pharmaceuticals: looking beyond intuition. *Science* **317**, 1881–1886 (2007).
5. O'Hagan, D. Understanding organofluorine chemistry. An introduction to the C–F bond. *Chem. Soc. Rev.* **37**, 308–319 (2008).
6. Hansch, C., Leo, A. & Taft, R. W. A survey of Hamm substituent constants and resonance and field parameters. *Chem. Rev.* **91**, 165–195 (1991).
7. Andreades, S. Fluorocarbanions. Rates of base-catalyzed hydrogen-deuterium exchange, isotope effects and acidity of monohydrofluorocarbons. *J. Am. Chem. Soc.* **86**, 2003–2010 (1964).
8. Wu, T. et al. Perfluoro-*tert*-butanol: a cornerstone for high performance fluorine-19 magnetic resonance imaging. *Chem. Commun.* **57**, 7743–7757 (2021).
9. Kiviniemi, A. & Virta, P. Characterization of RNA invasion by ^{19}F NMR spectroscopy. *J. Am. Chem. Soc.* **132**, 8560–8562 (2010).
10. Tirotta, I. et al. A superfluorinated molecular probe for highly sensitive in vivo ^{19}F-MRI. *J. Am. Chem. Soc.* **136**, 8524–8527 (2014).
11. Lagow, R. J., Shimp, L. A. & Clark. L. C., Jr. Fluorinated tetramethylpentane blood substitutes. US4187252, February 5, 1980.
12. Otomo. S. Fluorinated alkyl benzenes as corrosion and rust inhibitors. EP569884, November 18, 1993.
13. Takada, N., Abe, T. & Sekiya, A. Preparation and physicochemical properties of F-*tert*-butyl alkyl ethers. *J. Fluor. Chem.* **92**, 167–171 (1998).
14. Michelena, O., Padro, D., Carrillo-Carrión, C., del Pino, P., Blanco, J., Arnaiz, B., Parak, W. J. & Carril, M. Novel fluorinated ligands for gold nanoparticle labelling with applications in ^{19}F-MRI. *Chem. Commun.* **53**, 2447–2450 (2017).
15. Meng, H., Wen, L., Xu, Z., Li, Y., Hao, J. & Zhao, Y. Nonafluoro-*tert*-butoxylation of diaryliodonium salts. *Org. Lett.* **21**, 5206–5210 (2019).
16. Yagupolskii, Y. L. & Petko, K. I. N-perfluoro-*tert*-butylazoles. *J. Fluor. Chem.* **176**, 9–13 (2015).
17. Wang, L., Feng, Z., Luo, Z., Guo, Z., Wang, J. & Yi, W. Direct synthesis of *N*-perfluoro-*tert*-butyl secondary amines from *N*-trifluoromethyl secondary amines. *Chem. Sci*. https://doi.org/10.1039/D4SC06335J (2024).
18. Delyagina, N. I., Pervova, E. Y. & Knunyants, I. L. Reaction of perfluoro-tert-butyl carbanion with olefins, containing an activated double bond, and with three-membered heterocycles and various halo derivatives. *Russ. Chem. Bull.* **21**, 326–329 (1972).
19. Wang, Q. et al. Fluorination triggers fluoroalkylation: nucleophilic perfluoro-*tert*-butylation with 1,1-dibromo-2,2-bis(trifluoromethyl) ethylene (DBBF) and CsF. *Angew. Chem. Int. Ed.* **60**, 27318–27323 (2021).
20. Wei, Z., Wen, L., Zhu, K., Wang, Q., Zhao, Y. & Hu, J. Regioselective aromatic perfluoro-*tert*-butylation using perfluoro-*tert*-butyl phenyl sulfone and arynes. *J. Am. Chem. Soc.* **144**, 22281–22288 (2022).
21. Avila, D. V., Ingold, K. U., Lusztyk, J., Dolbier, W. R. & Pan, H. Q. Perfluoro-*tert*-butyl, a reactive, neutral, electrophilic carbon-centered radical par excellence. *Tetrahedron* **52**, 12351–12356 (1996).
22. Lloyd, R. V. & Rogers, M. T. Electron-spin resonance study of some perfluoroalkyl radicals. *J. Am. Chem. Soc.* **95**, 1512–1515 (1973).
23. Mochalina, E. P., Dyatkin, B. L., Galakhov, I. V. & Knunyant, I. L. Preparation of some compounds containing a perfluoro-tetrbutyl group. *Dokl. Akad. Nauk SSSR* **169**, 1346–1349 (1966).
24. Yajima, T., Yamaguchi, K., Hirokane, R. & Nogami, E. Photoinduced radical hydroperfluoroalkylation and the synthesis of fluorinated amino acids and peptides. *J. Fluor. Chem.* **150**, 1–7 (2013).
25. Dong, Z. & MacMillan, D. W. C. Metallaphotoredox-enabled deoxygenative arylation of alcohols. *Nature* **598**, 451–456 (2021).
26. Sakai, H. A. & MacMillan, D. W. C. Nontraditional fragment couplings of alcohols and carboxylic acids: C(sp^3)–C(sp^3) cross-coupling via radical sorting. *J. Am. Chem. Soc.* **144**, 6185–6192 (2022).
27. Intermaggio, N. E., Millet, A., Davis, D. L. & MacMillan, D. W. C. Deoxytrifluoromethylation of alcohols. *J. Am. Chem. Soc.* **144**, 11961–11968 (2022).
28. Lin, Q., Ma, G. & Gong, H. Ni-catalyzed formal cross-electrophile coupling of alcohols with aryl halides. *ACS Catal* **11**, 14102–14109 (2021).
29. Zheng, Y.-X., Gao, Y., Xiong, P. & Xu, H.-C. Unlocking HFIP for fluoroalkylation with molecular photoelectrocatalysis. *Angew. Chem. Int. Ed.* https://doi.org/10.1002/anie.202423241 (2025).
30. Dyatkin, B. L., Mochalina, E. P. & Knunyants, I. L. The acidic properties of fluorine-containing alcohols, hydroxylamines and oximes. *Tetrahedron* **21**, 2991–2995 (1965).
31. Abraham, M. H., Grellier, P. L., Prior, D. V., Duce, P. P., Morris, J. J. & Taylor, P. J. Hydrogen bonding. Part 7. A scale of solute hydrogen-bond acidity based on log K values for complexation in tetrachloromethane. *J. Chem. Soc., Perkin Trans.* **2**, 699–711 (1989).
32. Wu, Y., Jiang, Y., Wang, F., Wang, B. & Chen, C. Direct electrophilic and radical isoperfluoropropylation with *i*-C_3F_7-iodine(III) reagent (PFPI reagent). *Commun. Chem.* **6**, 177 (2023).
33. Ge, C., Wang, B., Jiang, Y. & Chen, C. Diverse reactivity of the gem-difluorovinyl iodonium salt for direct incorporation of the difluoroethylene group into *N*- and *O*-nucleophiles. *Commun. Chem.* **5**, 167 (2022).
34. Sheng, J. Y., Wang, Y., Su, X., He, R. & Chen, C. Copper-catalyzed [2+2+2] modular synthesis of multisubstituted pyridines: alkenylation of nitriles with vinyliodonium salts. *Angew. Chem. Int. Ed.* **56**, 4824–4828 (2017).
35. Bielawski, M., Zhu, M. & Olofsson, B. Efficient and general one-pot synthesis of diaryliodonium triflates: optimization, scope and limitations. *Adv. Synth. Catal.* **349**, 2610–2618 (2007).
36. Phipps, R. J., Grimster, N. P. & Gaunt, M. J. Cu(II)-catalyzed direct and site-selective arylation of indoles under mild conditions. *J. Am. Chem. Soc.* **130**, 8172–8174 (2008).
37. Allen, A. E. & MacMillan, D. W. C. Enantioselective alpha-arylation of aldehydes via the productive merger of iodonium salts and organocatalysis. *J. Am. Chem. Soc.* **133**, 4260–4263 (2011).
38. Toh, Q. Y., McNally, A., Vera, S., Erdmann, N. & Gaunt, M. J. Organocatalytic C–H bond arylation of aldehydes to bis-heteroaryl ketones. *J. Am. Chem. Soc.* **135**, 3772–3775 (2013).
39. Bielawski, M., Malmgren, J., Pardo, L. M., Wikmark, Y. & Olofsson, B. One-pot synthesis and applications of N-heteroaryl iodonium salts. *ChemistryOpen* **3**, 19–22 (2014).
40. Wang, G.-Z., Shang, R., Cheng, W.-M. & Fu, Y. Irradiation-induced Heck reaction of unactivated alkyl halides at room temperature. *J. Am. Chem. Soc.* **139**, 18307–18312 (2017).
41. Bellotti, P., Huang, H. M., Faber, T. & Glorius, F. Photocatalytic late-stage C–H functionalization. *Chem. Rev.* **123**, 4288–4289 (2023).
42. Straathof, N. J. W., Cramer, S. E., Hessel, V. & Noël, T. Practical photocatalytic trifluoromethylation and hydrotrifluoromethylation of styrenes in batch and flow. *Angew. Chem. Int. Ed.* **55**, 15549–15553 (2016).
43. Honeker, R., Garza-Sanchez, R. A., Hopkinson, M. N. & Glorius, F. Visible-light-promoted trifluoromethylthiolation of styrenes by dual photoredox/halide catalysis. *Chem. Eur. J.* **22**, 4395–4399 (2016).
44. Wei, X.-J., Boon, W., Hessel, V. & Noël, T. Visible-light photocatalytic decarboxylation of α,β-unsaturated carboxylic acids: facile access to stereoselective difluoromethylated styrenes in batch and flow. *ACS Catal* **7**, 7136–7140 (2017).
45. Nevesely, T., Wienhold, M., Molloy, J. J. & Gilmour, R. Advances in the E→Z isomerization of alkenes using small molecule photocatalysts. *Chem. Rev.* **122**, 2650–2694 (2022).
46. Yang, X.-J., Lin, J.-H. & Xiao, J.-C. $BrCF_2CN$ for photocatalytic cyanodifluoromethylation. *Nat. Commun.* **16**, 445 (2025).

47. Chen, S., Zou, S. & Xi, C. Photocatalyzed 2:2 coupling of styrene and $BrCF_2CO_2Me$: a facile synthesis of bis-difluoroacetylated hexestrol derivatives. *Chin. J. Org. Chem.* **43**, 1157–1167 (2023).
48. Flamigni, L., Barbieri, A., Sabatini, C., Ventura, B. & Barigelletti, F. Photochemistry and photophysics of coordination compounds: iridium. *Top. Curr. Chem.* **281**, 143–203 (2007).
49. Chu, L. & Qing, F.-L. Copper-mediated aerobic oxidative trifluoromethylation of terminal alkynes with Me_3SiCF_3. *J. Am. Chem. Soc.* **132**, 7262–7263 (2010).
50. Wu, Y., Jiang, Y., Wang, F., Wang, B. & Chen, C. Light promoted metal-free regio- and stereoselective isoperfluoropropylation of unactivated alkenes with an *i*-C_3F_7-iodine (III) reagent. *Org. Chem. Front.* **11**, 370–379 (2024).
51. Cao, H., Cheng, Q. & Studer, A. Radical and ionic *meta*-C–H functionalization of pyridines, quinolines, and isoquinolines. *Science* **378**, 779–785 (2022).
52. Haring, M., Balanna, K., Cheng, Q., Lammert, J. & Studer, A. Formal *meta*-C–H-fluorination of pyridines and isoquinolines through dearomatized oxazinopyridine intermediates. *J. Am. Chem. Soc.* **146**, 30758–30763 (2024).
53. Melder, J. J. et al. Rudolph, M. & Hashmi, A. S. K. Easy access to functionalized indolines and tetrahydroquinolines *via* a photochemical cascade cyclization reaction. *J. Am. Chem. Soc.* **146**, 14521–14527 (2024).
54. Coric, I., Müller, S. & List, B. Kinetic resolution of homoaldols via catalytic asymmetric transacetalization. *J. Am. Chem. Soc.* **132**, 17370–17373 (2010).
55. Zhang, S., Zhou, S., Qi, J., Jiao, L. & Guo, X. Time-resolved electron paramagnetic resonance spectrometer based on ultrawide single-sideband phase-sensitive detection. *Rev. Sci. Instrum.* **94**, 084101 (2023).
56. Wang, F., Wang, D., Mu, X., Chen, P. & Liu, G. Copper-catalyzed intermolecular trifluoromethylarylation of alkenes: mutual activation of arylboronic acid and CF_3^+ reagent. *J. Am. Chem. Soc.* **136**, 10202–10205 (2014).
57. Xu, J. et al. Copper-catalyzed trifluoromethylation of terminal alkenes through allylic C–H bond activation. *J. Am. Chem. Soc.* **133**, 15300–15303 (2011).
58. Hu, X.-S., He, J.-X., Zhang, Y., Zhou, J. & Yu, J.-S. Highly stereoselective positional isomerization of styrenes *via* acid-catalyzed carbocation mechanism. *Chin. J. Chem.* **39**, 2227–2233 (2021).
59. Huang, Z., Qin, J., Hu, Y., Zhu, S. & Chu, L. Radical alkylcyanation of 1,6-enynes with isonitriles as bifunctional reagents. *Org. Lett.* **26**, 10763–10768 (2024).

Acknowledgements

This work was supported by the National Natural Science Foundation (NNSF) of China (No. 22071129, received by C.C.). R.Z. thanks Mr. Ruiyang Gao (Fudan University) for helpful discussions.

Author contributions

R.Z. and Y.L. performed the synthesis and DFT calculations. S.Z. performed the EPR study. R.Z. and S.Z. wrote the manuscript, Y.L., Y.W., X.C., F.W. and Y.J. discussed. X.G. and C.C. guided the project.

Competing interests

R.Z. and C.C. may benefit from a patent relevant to this work (CN119143694A). The remaining authors declare no competing interests.

Additional information

Supplementary information The online version contains supplementary material available at https://doi.org/10.1038/s41467-025-59772-5.

Correspondence and requests for materials should be addressed to Xingwei Guo or Chao Chen.

Peer review information *Nature Communications* thanks Chengshuo Shen and the other anonymous reviewer(s) for their contribution to the peer review of this work. A peer review file is available.